Temperature effects in the magnetic properties of two-dimensional Ising square lattices: A Monte Carlo investigation

Yongyut Laosiritaworn,* Supon Ananta, and Rattikorn Yimnirun
Department of Physics, Faculty of Science, Chiang Mai University, Chiang Mai 50200, Thailand
(Received 3 November 2006; revised manuscript received 5 January 2007; published 22 February 2007)

The magnetic behavior of a two-dimensional nearest-neighbor Ising model with the presence of linear temperature variation in a thermal steady state was studied using the Wolff Monte Carlo simulation. The technique consists of fixing the temperatures of boundary spins, while the temperature field in the interior linearly varies with distance. It is found that with increasing the temperature difference between the two boundaries, the magnetization greatly reduces in magnitude while the susceptibility peaks tend to spread out over a temperature range. The detailed descriptions of these magnetization and susceptibility behaviors are elucidated from their spatial variation. The extraction of the "critical temperatures" is taken via the fourth-order cumulant of the magnetization. The critical temperatures are found to reduce slightly with increasing the temperature difference. This implies the vulnerability of the magnetization and susceptibility properties to the temperature variation in ferromagnetic materials, and to use such materials in temperature variation environments must be done with caution.

DOI: 10.1103/PhysRevB.75.054417 PACS number(s): 75.10.Dg, 05.10.Ln, 75.40.Cx

I. INTRODUCTION

Magnetic thin films have been known to be very important in terms of fundamental and technological interest, especially in the magnetic recording technology.[1,2] Many contributions have been taken to provide understanding of these systems in detail.[3,4] However, there are still incomplete pictures describing their magnetic properties especially in nonequilibrium states. For instance, the theoretical studies usually investigate the thin-film problems by considering the system in contact with only a single heat bath, which means that the temperature of the whole system is fixed. As a result, the conventional thermal equilibrium investigation may not be useful in understanding the magnetic materials used in some applications, which operate at some fluctuating temperatures. For instance, in heat-assisted magnetic recording, the media temperature is nonuniformly raised by laser irradiation.[5] In such applications, there occurs a heat flux flowing among regions from high to low temperatures, resulting in local variation in temperature. Therefore, the approximation on using a single (average) temperature in the calculation is clearly inadequate since important thermodynamics is missing. On the other hand, magnetic properties strongly depend on thermal fluctuation. Therefore, the variation in temperatures makes the problem very complex, so experimental and theoretical investigations of this issue cannot be taken trivially. Consequently, it is of great interest and challenge to find how magnetic properties respond to the variation in temperature field. To date, there are few studies on this effect of temperature variation on magnetic systems; i.e., they are mainly restricted to the thermal properties such as heat conductivity.[6,7] A particular study on the field uses nonequilibrium simulations to calculate thermal conductivity in a two-dimensional (2D) Ising system based on microcanonical algorithm,[8] which was later extended to include external magnetic field.[9]

Therefore, in this study, the understanding of the effect of temperature variation, but restricted only to thermal steady state, on magnetic system has been extended by performing Monte Carlo simulation to investigate magnetic properties, i.e., the magnetization and the magnetic susceptibility including their spatial resolution. The simulation considers the use of Ising model, which has been proven to be useful in many areas starting from biological systems[10,11] to financial problems[12,13] and statistical mechanics, with the ultrathin film or 2D structure. Also, in magnetic material problems, both theoretical[14,15] and experimental investigations[16–18] have also shown, in terms of critical exponents, that the 2D Ising system is very useful for the study of magnetic behavior in thin ferromagnetic films. To outline, the study investigates how the overall average magnetic properties, such as the magnetization and the magnetic susceptibility, depend on temperature supplied to the boundary spins from the heat baths and heat bath temperature differences by means of Monte Carlo simulations. Next, the study investigates the variation of these magnetic properties in terms of spatial resolution to observe how local magnetic behavior plays a part in overall average magnetic properties. Then, the "critical temperature," which is defined to be the temperature (of a lower temperature heat bath) where the order parameter of the system vanishes at thermodynamic limit, is extracted to examine how the temperature variation affects the critical phenomena. These are followed by a conclusion, which summarizes a prominent finding from the study, and a suggestion on how the topic would benefit the community.

II. METHODOLOGY

In this study, we consider the Ising Hamiltonian

$$H = -J\sum_{\langle ij\rangle} S_i S_j, \tag{1}$$

where the spins $S_{i(j)}$ take on the values ± 1 and the sum includes only first nearest-neighbor pairs. The units J and J/k_B are used for temperatures and energies, respectively. The

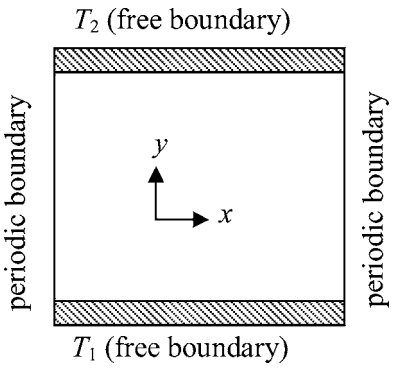

FIG. 1. The setup system structure showing its boundary conditions and its temperature constraint on the free boundaries, i.e., T_1 at $y=1$ and T_2 at $y=L$, where $T_1 \leqslant T_2$.

considered system is a 2D structure where periodic and free boundary conditions are used for the x and y directions, respectively. The simulations are carried out with total number of spins $N=L_x \times L_y$, where L_x and L_y represent the number of magnetic (atomic) sites along the x and y directions of the system. A rule of thumb in performing Monte Carlo simulations is to choose L_x and L_y as large as possible to minimize finite-size effect. Therefore, in this study we use $L_x=L_y=L$ ranging from 40 to 100 in steps of 10, which are still computationally feasible and fairly large. Actually, these chosen L are picked from the L that the correction to scaling is not significantly needed in the investigation of critical properties.[19] In fact, the finite-size effect causes the deviation in any physical properties between those of the finite system and of the infinite system especially close to critical point. This can be described using the critical behavior of the magnetic interaction. For instance, in a paramagnetic phase, the correlation length of the same spin is small. However, on approaching the critical point from above, the correlation length starts to grow and blows up if the considered system is very large (L tends to infinity). Nevertheless, for finite L, the divergence of the correlation length is not permitted since the largest value of the correlation length itself is L. Furthermore, due to finite-size effect, which arises from the free surfaces (if there are any), or the periodic image (if the periodic boundary condition is chosen), the rate of correlation growing in the finite-size system and the infinite system is different, and this alters the magnetic properties in the finite system from the infinite system. For example, it is very obvious that the magnetization in the finite system does not cease down to zero at the critical point.

Next, in applying temperatures to the system, along the y direction, at $y=1$ and L_y, the fixed temperatures T_1 and T_2 where $T_1 < T_2$ (see Fig. 1) are supplied to the boundary spins. Due to the temperature variation, starting from the $y=1$ side, the temperature steadily increases from T_1 and reaches T_2 at the opposite side. In this nonequilibrium state, the heat flux passes from the T_2 side to the T_1 side, while local temperatures along the pathway can be determined from the heat conduction formula,

$$\frac{1}{A}\frac{dQ}{dt} = -K\frac{dT}{dx}, \tag{2}$$

where K is the thermal conductivity and dT/dx refers to the one-dimensional temperature gradient. However, when the system relaxes to its steady state, the ratio dQ/dt is maintained and the resulting temperature gradient becomes a constant. As a result, at this steady state, the temperature T is linearly proportional to the distance away from the T_1 side and it can be estimated that

$$T_y = T_1 + \left(\frac{T_2 - T_1}{L_y - 1}\right)y, \tag{3}$$

where y is the distance away from T_1 and T_y is the local temperature at y. Because the study considers the system only in its steady state, the local temperature T_y is therefore fixed at the distance y throughout the simulation, giving rise to various local thermal equilibria for each specific distance y in the system.

In this study, we consider the temperature difference between the two heat baths $\Delta T=T_2-T_1$ ranging from 0.0 to 2.8 J/k_B with steps of 0.4 J/k_B, and T_1 ranging from 0.1 to 3.4 J/k_B with steps of 0.1 J/k_B. With these ΔT and T_1 ranges, it is possible to investigate the system in several cases. For instance, both T_1 and T_2 are in ferromagnetic phase, T_1 is in ferromagnetic but T_2 is in paramagnetic phase, and both T_1 and T_2 are in paramagnetic phase. Note that without temperature variation, the 2D Ising critical temperature T_C, which splits paramagnetic out of ferromagnetic phase, is $T_C=2/\ln(1+\sqrt{2}) \approx 2.269\ J/k_B$.[20]

Next, in updating the spin configurations during Monte Carlo simulations, a series of successive spin configurations are chosen via importance sampling under the condition of ergodicity and detailed balance. A very popular algorithm, which satisfies these conditions, is the Metropolis algorithm,[21] where a particular spin configuration is different from its previous configuration by only a single spin flip. The probability in accepting a new spin configuration, which is generated from the previous study, is $p=\exp(-\Delta E/k_B T_y)$, where ΔE is the energy difference associated with the flip and T_y is the local temperature attached to the flipped spin. However, instead of using the conventional Metropolis algorithm, we consider the Wolff algorithm[22] because the Wolff greatly reduces the correlation time τ. This is due to the fact that the updated probability in Metropolis algorithm depends only on an energy difference from a single spin flip. Therefore, this results in a large correlation time τ among successive spin configurations.[23,24] In the following, the large τ brings a large statistical error of the magnetization $\langle(\delta m)^2\rangle$ because[23,24]

$$\langle(\delta m)^2\rangle = \frac{1}{n}(\langle m^2\rangle - \langle m\rangle^2)\left(1 + 2\frac{\tau}{\delta t}\right), \tag{4}$$

where, at large enough n, $\tau=\Sigma(\langle m_0 m_i\rangle - \langle m^2\rangle)/(\langle m^2\rangle - \langle m\rangle^2)$ is the integrated correlation time and δt is the time interval between two successive configurations, and n is the number of configurations being sampled. As can be seen from the above equation, the smaller the τ, the lower the statistical

error. Therefore, one can see the benefit of using the Wolff algorithm upon the Metropolis algorithm since the Wolff provides a smaller τ in the same system. For example, close to critical temperature in 2D Ising model, the correlation time τ scales with the system size L as $\tau \propto L^z$, and the gives $z=0.25\pm0.01$,[25] while the Metropolis gives $z=2.1665\pm0.0012$.[26]

In using the Wolff algorithm to make configuration updates, a cluster of the same direction spins is made and flipped. In creating the cluster, a seed spin is randomly chosen and then its neighboring spins, at temperature T_y, are added to form a group with a probability

$$p = 1 - \exp\left(-\frac{2J}{k_B T_y}\right). \tag{5}$$

Then, the procedure is repeated for the just added spins until no more spins are added to the cluster. Next all the spins in the cluster are flipped to their opposite directions, i.e., S_i to $-S_i$.

In this Monte Carlo study, with the chosen Wolff algorithm, we first waited for each simulation at least for 1000 Monte Carlo steps per site (MCS) from its initial state (disordered state) to allow the system to relax to its steady state before taking any measurements. After that, during the simulation, the magnetization and the energy are measured when the number of flipped spins exceeds or is equal to N. The global average of the magnetization per spin is defined as $m=(1/N)\Sigma_i S_i$, and in each simulation, $N'=50\,000$ configurations are used to calculate the expectation of the magnetization per spin, i.e.,

$$\langle m \rangle = \frac{1}{N'} \sum_{t}^{N'} |m_t|. \tag{6}$$

It is also of interest to observe how the free boundaries play their roles on the microscopic magnetic properties. This is so since the effect of average exchange interaction on a single magnetic spin strongly depends on its neighboring. At the free boundary, the smaller number of nearest-neighbor sites causes the smaller magnitude of average exchange interaction, whereas in the interior the spin feels more bulklike (homogeneously). So the variation of magnetic properties from the free boundary to the interior of the system is expected. Therefore, the spatial dependence of the magnetic properties, i.e., m_y and χ_y, for distance y away from the T_1 side, is calculated to observe the free boundary effect (for which the temperature variation is not yet turned on) and the temperature variation effects on the local magnetic properties. Specifically, the study considers the variation of m_y and χ_y as a function of the distance y away from the T_1 side to the direction toward the T_2 side. For convenience, only y that is a multiple of lattice spacing unit is considered, and all spins at the same distance y are defined to have local magnetization and local susceptibility per spins in the absence of external field as $m_y=(1/L)\Sigma_{i\in y} S_i$ and $\chi_y=L(\langle m_y^2\rangle - \langle m_y\rangle^2)/k_B T_y$. Note that we have applied the thermal equilibrium formalism to microscopically investigate the thermal steady state because all spins at the same distance y are virtually attached to the same heat bath at temperature T_y. In this way, it means that we first consider the region to be small enough to experience only a single and stable temperature, and then the thermal equilibrium technique is applied to study this microscopic region. After that, the dependence of the magnetic properties on the spatial temperature is calculated and the overall magnetic properties are extracted by averaging the microscopic properties. Note that if the system has not yet arrived at the steady state, everywhere except at the boundary the spins we will notice the spatial temperatures to change in time and the thermal equilibrium technique cannot be applied to such case.

Next, based on the local magnetic susceptibility χ_y, the global (average) magnetic susceptibility at zero field is defined as

$$\chi \equiv \left.\frac{\partial m}{\partial h}\right|_{h\to 0} = \frac{1}{L}\sum_y \left.\frac{\partial m_y}{\partial h}\right|_{h\to 0} = \frac{1}{L}\sum_y \chi_y$$

$$= \sum_y \frac{1}{k_B T_y}(\langle m_y^2\rangle - \langle m_y\rangle^2). \tag{7}$$

Also in this study, the critical behavior is investigated via the critical temperature T_C. Note that the term critical temperature used in this context is the temperature that the magnetization of the whole system vanishes at the thermodynamic limit. In this temperature variation study, at a particular temperature, some parts of the system may already lie in paramagnetic state, but if there are still some other parts residing in ferromagnetic state, the whole system is categorized to be ferromagnetic since there still exists finite magnetization. Then, T_C is defined if and only if the magnetization is completely destroyed by the thermal fluctuation that spreads throughout the system (in the infinite sized system). However, due to computational limitation, the simulations have to be performed in finite sizes where their finite-size effects must be taken into account. Therefore, in this study, the temperature T_C is phenomenologically located via the fourth-order cumulant U_L of the magnetization per spin,[27]

$$U_L = 1 - \frac{\langle m^4\rangle}{3\langle m^2\rangle^2}, \tag{8}$$

where, at critical point, U_L should be independent of L; i.e., for differing sizes L and L', $(U_L/U_{L'})_{T=T_C}=1$. The reason in using Eq. (8), which was created to study thermal equilibrium systems to extract the critical temperature T_C, is based on the fact that the correlation length of the magnetization diverges (or the spontaneous symmetry breaking occurs throughout the system) at the critical point. Thus, no matter how large the system size L is, U_L should be the same at the critical point. Therefore, in this study of thermal steady state, for a specific value of ΔT, the critical temperature is defined in terms of T_1 (the lower temperature heat bath), which allows the correlation length of global magnetization to diverge at the thermodynamic limit and results in $(U_L/U_{L'})_{T=T_C}=1$. In fact, instead of T_1, one may define the critical temperature in terms of T_2 if it is desired. However, in this study, the lower temperature of the two heat baths is

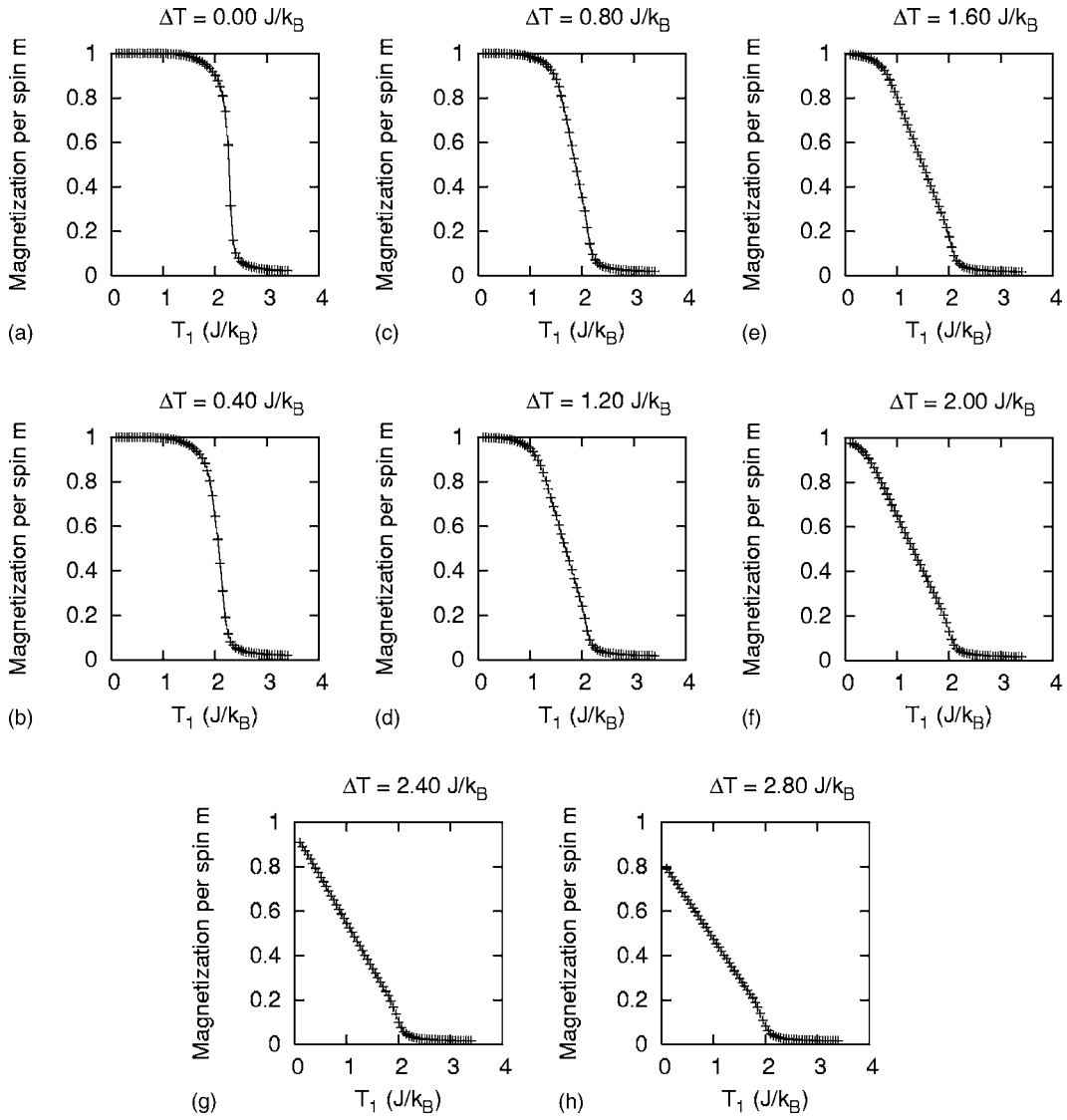

FIG. 2. Magnetization per spin m as a function of temperature T_1 for various $\Delta T = T_2 - T_1$.

preferred to define the critical temperature.

Nevertheless, owing to finite-size effects, the cumulant curves obtained from Eq. (8) for different L's do not exactly cross at the same temperature. Therefore, the critical temperature is estimated from $T_C(b=L/L')$ at the limit $(\ln b)^{-1} \to 0$.[24,27] To maximize the efficiency of this T_C calculation, for each system, a single long simulation is only performed at a temperature T_0 and the histogram method[28,29] is used to extrapolate U_L to a temperature nearby in order to find the cumulant crossing points on a fine scale. The temperature T_0 is guessed from the temperature at the center of the cumulant crossing points. Approximately 2×10^5 spin configurations, which are found to compromise between calculation time and statistical error, are used to create the histograms. To exclude the data obtained from temperatures too far from the simulated temperature T_0, the range of the extrapolation obeys $|U(T) - U(T_0)| \leq \sigma_E$, where $U = \langle E \rangle$ is the average of the energy and σ_E is a standard deviation of E at T_0.[30]

III. RESULTS AND DISCUSSIONS

A. Overall magnetization and magnetic susceptibility profiles

From the simulations, the magnetization m and susceptibility χ profiles for various T_1 and temperature difference $\Delta T = T_2 - T_1$ are obtained and shown in Figs. 2 and 3. As can be seen from Fig. 2, with increasing ΔT, the magnetization m tends to decrease. This is because the larger ΔT is, the greater the temperature is at the hotter part of the system (close to the T_2 side). Then, at this hotter part, the magnetic spins experience larger thermal fluctuation, resulting in smaller local magnetization magnitude. Consequently, on the overall average, the magnetization reduces with increasing ΔT. Note that even the magnetization significantly reduces in magnitude at large ΔT, the critical point (the temperature where magnetization curve has the maximum slope) only slightly changes. This is due to the fact that there are still some parts of the system, connecting to lower temperature T_1, which reside in ferromagnetic phase even magnetic order

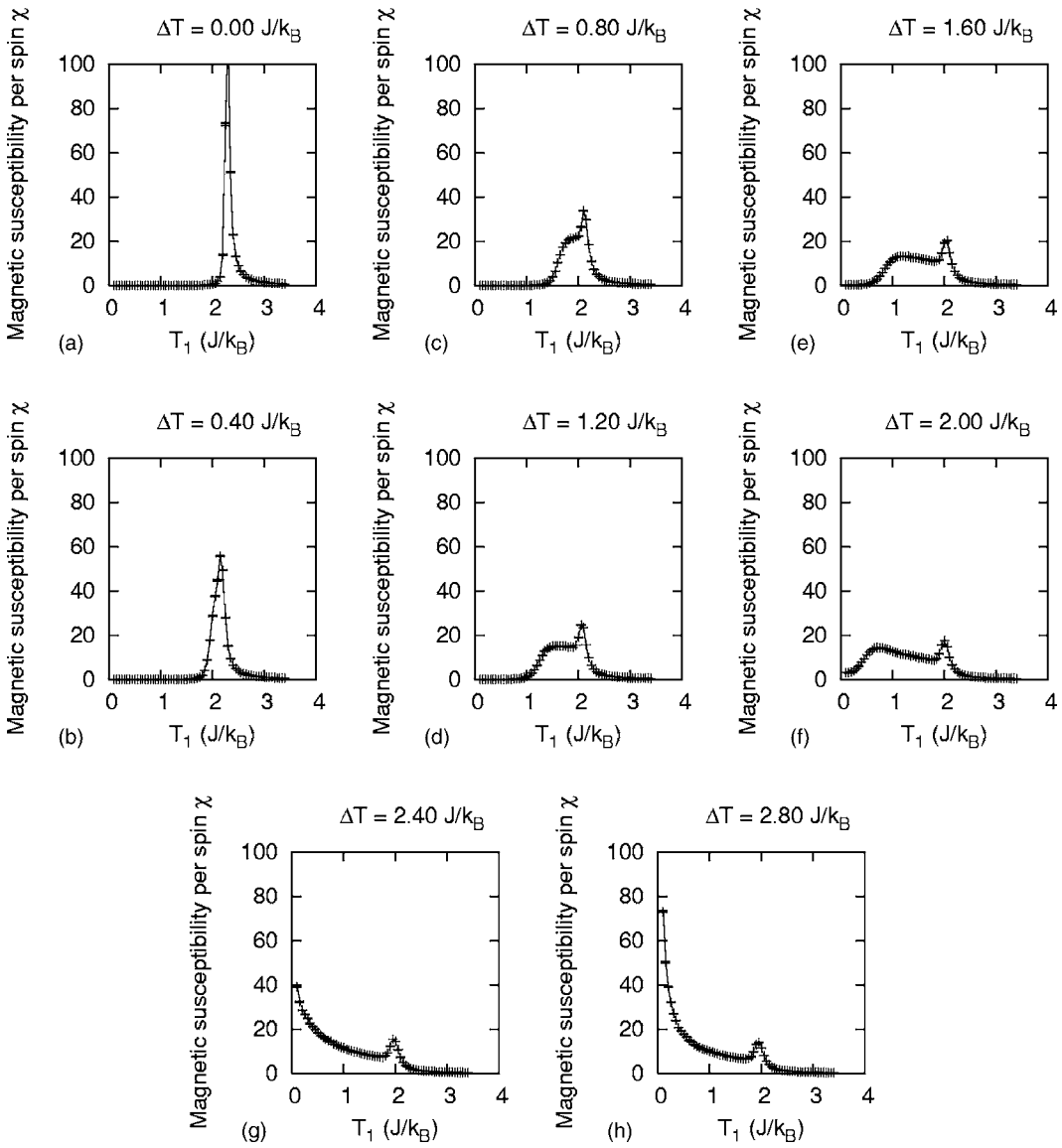

FIG. 3. Magnetic susceptibility per spin χ as a function of temperature T_1 for various $\Delta T = T_2 - T_1$.

of the other parts has already been destroyed. Therefore, the whole system presents some finite magnetization and preserves the overall ferromagnetic behavior. This phenomenon is similar to those found in magnetic thin films where exchange interaction varies from layer to layer.[31] In Ref. 31, because of the differences in exchange interaction magnitude, the magnetic orders from different layers are not destroyed at the same temperature. Therefore, the true critical temperature is defined to be the largest eigenvalue (temperature) that allows the susceptibility to diverge (under the framework of mean-field theory), which is the first encounter of temperature in which the overall magnetization is completely destroyed by the thermal fluctuation if the system is heated from its ferromagnetic phase.

On the other hand, the results for magnetic susceptibility χ, as in Fig. 3, show a broader range of phase transition for $\Delta T > 0$. This is very different from the case $\Delta T = 0$ where the susceptibility blows up only at the normal 2D Ising critical temperature $T_C \approx 2.269\ J/k_B$. This is due to the fact that the susceptibility is representative of magnetization fluctuation which severely increases in magnitude at the critical point. As for $\Delta T > 0$, there is temperature variation, making the temperature field rise in magnitude from T_1 to T_2. Consequently, different parts of the system experience different local temperatures. Some parts may already reach the critical point where others may not. Each part of the system will not highlight the critical behavior at the same temperature T_1. For example, at $T_1 = 1.60\ J/k_B$ and $\Delta T = 0.6\ J/k_B$, the spins close to the T_1 boundary are lying in ferromagnetic state and their local susceptibility will be very small. On the other hand, the spins close to the $T_2 = 2.00\ J/k_B$ boundary will start to exhibit large thermal induced magnetization fluctuation since this temperature T_2 is close to T_C. Therefore, the local susceptibility for spins close to T_2 will be fairly large. Another example is the case where $T_1 = 2.20\ J/k_B$ and $\Delta T = 0.2\ J/k_B$. The local susceptibility will be large for spins close to T_1, but will be small for spins close to T_2 because these spins are already lying in paramagnetic state. These two examples

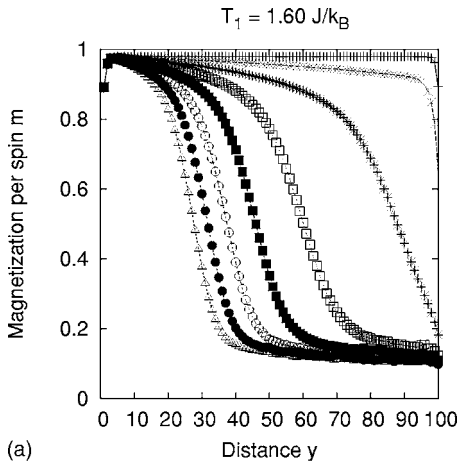

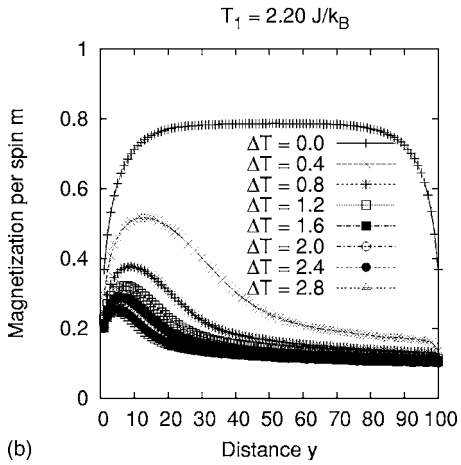

FIG. 4. Spatial variation of magnetization per spin m as a function of distance y away from the T_1 boundary for various ΔT at (a) $T_1=1.60\ J/k_B$ and at (b) $T_1=2.20\ J/k_B$. The legends to symbols in (a), which are the same as those in (b), are removed for visual aids.

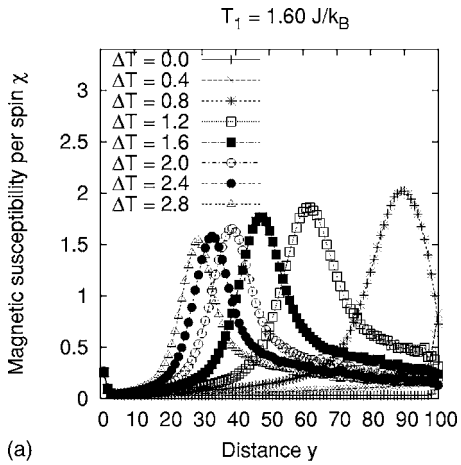

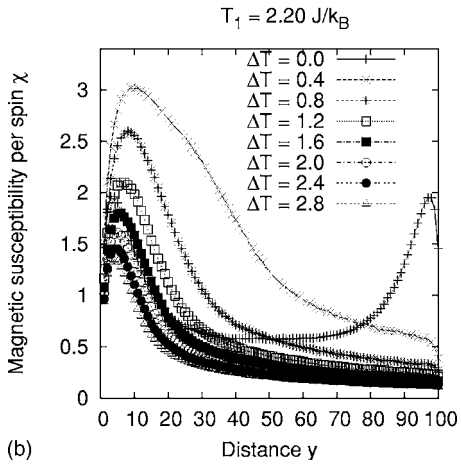

FIG. 5. Spatial variation of magnetic susceptibility per spin χ as a function of distance y away from the T_1 boundary for various ΔT at (a) $T_1=1.60\ J/k_B$ and at (b) $T_1=2.20\ J/k_B$.

can be used to describe the susceptibility phenomena in Fig. 3. Even T_1 is smaller than the normal 2D T_C, but with help from ΔT, there will be some interior parts of the system which will exhibit critical behavior. This results in a broader range of the susceptibility peak on the temperature T_1 scale. Nevertheless, the peak is not as sharp as the $\Delta T=0\ J/k_B$ system because in the case of $\Delta T=0\ J/k_B$, all spins contribute in magnetization fluctuation at the same temperature, i.e., T_C. A more detailed description of this broader range can be given by looking at spatial variation of the magnetic properties (see Figs. 4 and 5).

B. Spatial variation of magnetization and magnetic susceptibility

The study has found that the temperature variation has a strong effect on the local (spatial) magnetic properties. For example, Fig. 4 shows the spatial variation of magnetization per spin m as a function of distance y away from the T_1 boundary for various temperature differences $\Delta T=0.0$, 0.4, 0.8, 1.2, 1.6, 2.0, 2.4, and 2.8 J/k_B at (a) $T_1=1.60\ J/k_B$ and at (b) $T_1=2.20\ J/k_B$. Starting with $\Delta T=0\ J/k_B$, all spins experience the same temperature throughout the system. All parts of the system have the same magnetic behavior; i.e., all local magnetization and local susceptibility show the critical behavior at the same T_C, which is about 2.269 J/k_B for normal infinite size 2D Ising system. The spins on both T_1 and T_2 boundaries have a lower magnetization magnitude than those from other spins in the interior (see Fig. 4). This is due to the fact that the spins inside are coupled with four nearest-neighbor spins, while spins at the edges ($y=1$ and $y=L$) experience the free boundary and are coupled with only three nearest-neighbor spins. Therefore, the spins close to the T_1 and T_2 boundaries are more susceptible to the thermal fluctuation and result in a smaller magnetization magnitude. On the other hand, the spins which reside in the interior experience a higher level of ferromagnetic interaction, causing more spins to point to the same direction and yield a higher magnitude of magnetization. These results agree well with previous Ising model investigations that the spins at the free boundaries have smaller magnetization magnitudes compared with those in the interior.[32,33]

However, with increasing $\Delta T>0$, the temperature variation induced by temperature gradient in the system linearly raises the temperature T from the T_1 boundary to T_2 boundary. This makes the local magnetic properties vary, which is

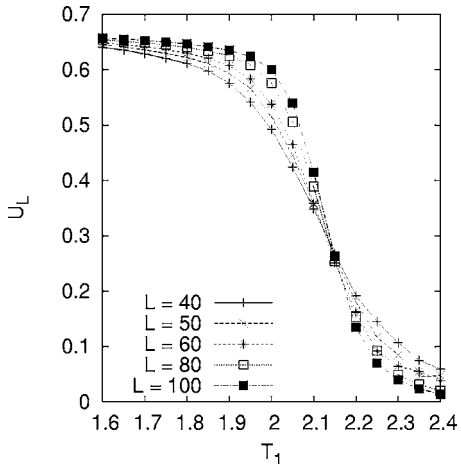

FIG. 6. The fourth-order cumulant of the magnetization for $\Delta T=1.20\ J/k_B$ system as a function of T_1. From the figure, it can be estimated that the crossing points take place between $T_1=2.10$ and $2.20\ J/k_B$, therefore, the critical temperature will lie in this region.

very different from the $\Delta T=0$ case. Looking at Fig. 4(a) as an example, at $T_1=1.60\ J/k_B$ and $\Delta T<0.669\ J/k_B$, both T_1 and T_2 are smaller than the normal $T_C\approx 2.269\ J/k_B$, and the whole system experiences ferromagnetic coupling. Therefore, finite magnetization behavior can be found throughout the system. Nevertheless, the magnetization reduces in magnitude from the T_1 boundary to the T_2 boundary due to a higher level of thermal fluctuation. On the other hand, for $\Delta T>0.669\ J/k_B$, the spins at and close to the T_2 boundary experience paramagnetic interaction because T_2 is greater than the normal 2D Ising T_C. Consequently, the magnetization reduces very sharply from the T_1 to the T_2 boundary. This detailed description can also be applied to understand the magnetization behavior in Fig. 4(b). Therefore, these are the reasons why the magnetization declines with increasing ΔT (e.g., see Fig. 2), which could be very useful in designing sensor applications such as the temperature sensor from magnetic materials.[34] In addition, as one may see in Fig. 4, the distance y away from the T_1 boundary is a "thermometer," which indicates the rise of temperature from T_1 to T_2. This is why the results in Fig. 4 are more or less similar to some subfigures in Fig. 2. Note that the magnetization does not completely reduce to zero because of the finite-size effect.

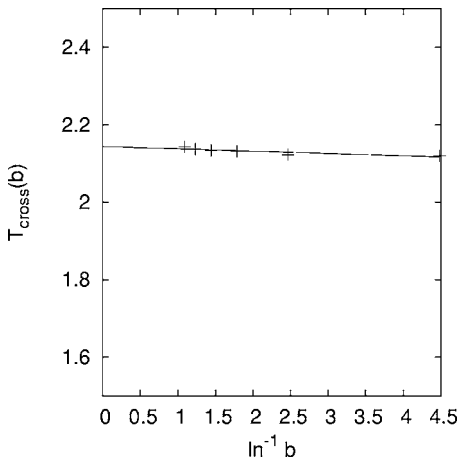

FIG. 7. The extraction of critical temperature T_C for $\Delta T=1.20\ J/k_B$ via the extrapolation of $T_{cross}(b)$ to the limit $\ln^{-1}(b)\rightarrow 0$, where T_{cross} is the temperature that $U_L=U_{L'}$ where $L'=40$ and $L=50$, 60, 70, 80, 90, and 100, and $b=L/L'$. The line is drawn from linear least-squares fit, which gives $T_C=2.14393\pm 0.00393\ J/k_B$.

TABLE I. Critical temperature T_C obtained from Monte Carlo simulation for various temperature differences between the two free boundaries.

$\Delta T=T_2-T_1$	T_C
0.0	2.26926±0.00018
0.4	2.19187±0.00312
0.8	2.16802±0.00273
1.2	2.14393±0.00393
1.6	2.13046±0.00367
2.0	2.11466±0.00406
2.4	2.09977±0.00640
2.8	2.08514±0.00510

Apart from the magnetization results, the temperature variation has a similar effect on the spatial magnetic susceptibility. For instance, at $\Delta T=0$ in Fig. 5(a), the whole system experiences the same temperature $T=T_1=T_2=1.60\ J/k_B$, which is smaller than T_C. The system is then far from the critical point and the thermally induced magnetization fluctuation (the susceptibility) is small. However, for $\Delta T=0$ in Fig. 5(b), the temperature $T=T_1=T_2=2.20\ J/k_B$ is close to T_C, so the magnetization starts to fluctuate strongly and the susceptibility starts growing (resulting in peaks) near the boundary T_1 and T_2 ends. In this $\Delta T=0$ case, the interior spins have a smaller susceptibility because there are more (average) number of neighbor spins which provides a higher magnetic interaction, and this interaction behaves as a buffer to the magnetization fluctuation. Similar to magnetization results, for $\Delta T>0$, the distance y indicates the rise of temperature. In Fig. 5, with increasing ΔT, the susceptibility peaks move toward the T_1 boundary since some parts inside the system have already reached T_C and this T_C moves towards the T_1 end with increasing ΔT.

C. Critical temperatures

On the other hand, in looking at the critical property, i.e., T_C, the fourth-order cumulant in Eq. (8) is found useful. The crossing of U_L is found for the whole range $\Delta T=0.0$–$2.8\ J/k_B$ in this study. An example for the cumulant crossing for $\Delta T=1.2\ J/k_B$ is shown in Fig. 6. As mentioned earlier, to minimize the finite-size effect, an extrapolation of $T_C(b=L/L')$ to the limit $(\ln b)^{-1}\rightarrow 0$ is performed (e.g., see Fig. 7). The critical temperatures T_C at this thermodynamic limit are presented in Table I and plotted as a function of temperature difference $\Delta T=T_2-T_1$ (see Fig. 8). As can been seen, for $\Delta T=0$ which is in the absence of temperature variation, the value of T_C agrees well with the exact solution, which is about $2.269\ J/k_B$ for normal infinite size 2D Ising model. This definitely assures the validity of the simulation codes.

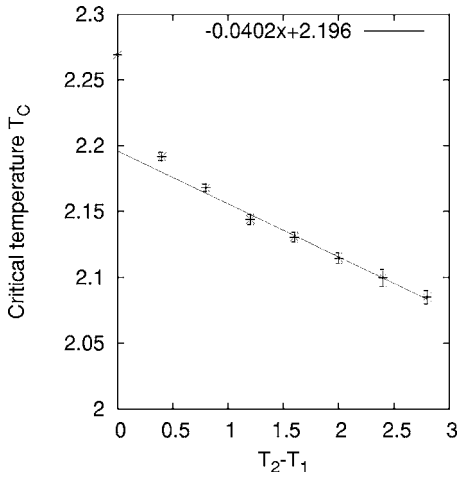

FIG. 8. Critical temperatures T_C obtained from 2D Ising simulations for various $\Delta T = T_2 - T_1$. The straight line is a linear least-squares fit to the data for $T_2 - T_1 \geqslant 0.8\ J/k_B$.

However, for $\Delta T > 0$, T_C reduces very sharply from $\Delta T = 0$ to $\Delta T = 0.8\ J/k_B$ and afterward reduces slightly for $\Delta T > 0.8\ J/k_B$. As can be seen in Fig. 8, it is possible to assign a linear fit to T_C for the range $\Delta T > 0.8\ J/k_B$, which gives $T_C(\Delta T) = -0.0402(\Delta T) + 2.196$. As evident from the linear fit in Fig. 8, the slope to the fitted function $dT_C/d(\Delta T) = -0.0402$ is rather small. This indicates that even if T_C reduces with increasing ΔT, it does not significantly change in magnitude. This implies that the temperature variation has some minor effects on the critical point by shifting T_C to a smaller value with increasing ΔT. This is so since the greater temperature difference brings more thermal fluctuation into the system so the transition from a ferromagnetic state to the parameter magnetic state occurs at a lower temperature. However, the change is not substantial because the paramagnetic state is defined for a magnetic state that all finite magnetizations are destroyed. Nevertheless, though the temperature variation brings a higher thermal fluctuation to the T_2 boundary causing the spins to align randomly and the local average magnetization close to this T_2 ceases down to zero, the spins close to the lower temperature side T_1 is still intact to the heat bath T_1 with a temperature smaller than the normal T_C. Therefore, some parts of the system still lie in ferromagnetic state. Hence, the overall average magnetization is not completely destroyed resulting in finite magnetization. As a result, unlike other magnetic properties, such as the sharp reduction in magnetization magnitude and the spreading out of susceptibility peaks over a temperature range, T_C changes very slightly.

IV. CONCLUSION

In this study, the effects of linear temperature variation on magnetic properties, i.e., the magnetization, the magnetic susceptibility, and the critical temperature, in the thermal steady state are investigated. In the absence of temperature difference ($\Delta T = 0$ or $T_1 = T_y = T_2$), the result (e.g., T_C) was found to agree well with the theoretical exact solution of the thermal equilibrium 2D Ising problem. This assures the validity of the simulation codes. However, when the temperature variation is turned on, the temperature difference at the boundaries supplies thermal fluctuation to the spins in the system with different magnitudes, and this makes the magnetization and the susceptibility become spatially dependent. The hotter and the colder parts of the system tend to show paramagnetic and ferromagnetic behaviors, respectively. The interference between these two behaviors turns out to be the reason why the average magnetization sharply reduces and the susceptibility peak becomes broader, while the critical temperature slightly decreases with increasing the temperature difference. The detailed descriptions of the phenomena are given via the investigation of spatial variation of the corresponding magnetic properties. To conclude, the study provides a detailed understanding of how the magnetic properties behave in response to the temperature variation in thermal steady state in ultrathin film, which may be another step closer in modeling real magnetic materials.

ACKNOWLEDGMENTS

The authors would like to acknowledge the Commission on Higher Education (Thailand) and the Thailand Research Fund for financial support.

*Corresponding author. FAX: +66 53 943445. Email address: yongyut_laosiritaworn@yahoo.com

[1] A. Moser, K. Takano, D. T. Margulies, M. Albrecht, Y. Sonobe, Y. Ikeda, S. Sun, and E. E. Fullerton, J. Phys. D **35**, r157 (2002).
[2] T. Osaka, T. Asahi, J. Kawaji, and T. Yokoshima, Electrochim. Acta **50**, 4576 (2005).
[3] P. J. Jensen and K. H. Bennemann, Surf. Sci. Rep. **61**, 129 (2006).
[4] F. Aguilera-Granja and J. L. Morán-López, Solid State Commun. **74**, 155 (1990).
[5] Shengbin Hu, Baoxi Xu, Hongxing Yuan, Yunjie Chen, Jun Zhang, and Rong Ji, J. Magn. Magn. Mater. **303**, e62 (2006).
[6] R. Harris and M. Grant, Phys. Rev. B **38**, 9323 (1988).
[7] M. Neek-Amal, R. Moussavi, and H. R. Sepangi, Physica A **371**, 424 (2006).
[8] M. Creutz, Phys. Rev. Lett. **50**, 1411 (1983).
[9] S. S. Mak, Phys. Lett. A **196**, 318 (1995).
[10] S. V. Buldyrev, N. V. Dokholyan, A. L. Goldberger, S. Havlin, C.-K. Peng, H. E. Stanley, and G. M. Viswanathan, Physica A **249**, 430 (1998).
[11] H. E. Stanley, S. V. Buldyrev, A. L. Goldberger, Z. D. Goldberger, S. Havlin, R. N. Mantegna, S. M. Ossadnik, C.-K. Peng, and M. Simons, Physica A **205**, 214 (1994).
[12] D. Horváth, M. Gmitra, and Z. Kuscsik, Physica A **361**, 589 (2006).
[13] A. Krawiecki and J. A. Hołyst, Physica A **317**, 597 (2003).

[14] K. Binder and P. C. Hohenberg, Phys. Rev. B **9**, 2194 (1974).
[15] M. Bander and D. L. Mills, Phys. Rev. B **38**, 12015 (1988).
[16] Y. Li and K. Baberschke, Phys. Rev. Lett. **68**, 1208 (1992).
[17] H. J. Elmers, J. Hauschild, H. Höche, U. Gradmann, H. Bethge, D. Heuer, and U. Köhler, Phys. Rev. Lett. **73**, 898 (1994).
[18] M. J. Dunlavy and D. Venus, Phys. Rev. B **69**, 094411 (2004).
[19] A. M. Ferrenberg and D. P. Landau, Phys. Rev. B **44**, 5081 (1991).
[20] B. M. McCoy and T. T. Wu, *The Two-Dimensional Ising Model* (Harvard University Press, Cambridge, MA, 1973).
[21] N. Metropolis, A. W. Rosenbluth, M. N. Rosenbluth, A. H. Teller, and E. Teller, J. Chem. Phys. **21**, 1087 (1953).
[22] U. Wolff, Phys. Rev. Lett. **62**, 361 (1989).
[23] H. Müller-Krumbhaar and K. Binder, J. Stat. Phys. **8**, 1 (1973).
[24] K. Binder and D. W. Heermann, *Monte Carlo Simulation in Statistical Physics* (Springer-Verlag, Berlin, 1992).
[25] P. D. Coddington and C. F. Baillie, Phys. Rev. Lett. **68**, 962 (1992).
[26] M. P. Nightingale and H. W. J. Blöte, Phys. Rev. Lett. **76**, 4548 (1996).
[27] K. Binder, Z. Phys. B: Condens. Matter **43**, 119 (1981).
[28] A. M. Ferrenberg and R. H. Swendsen, Phys. Rev. Lett. **61**, 2635 (1988).
[29] A. M. Ferrenberg and D. P. Landau, Phys. Rev. B **44**, 5081 (1991).
[30] M. E. J. Newman and G. T. Barkema, *Monte Carlo Methods in Statistical Physics* (Clarendon, Oxford, 1999).
[31] S. S. A. Razee, J. B. Staunton, L. Szunyogh, and B. L. Györffy, Phys. Rev. B **66**, 094415 (2002).
[32] Q. Hong, Phys. Rev. B **41**, 9621 (1990).
[33] Y. Laosiritaworn, J. Poulter, and J. B. Staunton, Phys. Rev. B **70**, 104413 (2004).
[34] H. Osada, S. Chiba, H. Oka, H. Hatafuku, N. Tayama, and K. Seki, J. Magn. Magn. Mater. **272-276**, e1761 (2004).